Stable isotope analysis of intact oxyanions using electrospray Quadrupole-Orbitrap mass spectrometry

Journal:	*Analytical Chemistry*
Manuscript ID	ac-2019-044864.R1
Manuscript Type:	Article
Date Submitted by the Author:	n/a
Complete List of Authors:	Neubauer, Cajetan; California Institute of Technology, Division of Geological and Planetary Sciences Crémière, Antoine; California Institute of Technology, Division of Geological and Planetary Sciences Wang, Xingchen; California Institute of Technology, Division of Geological and Planetary Sciences Thiagarajan, Nivedita; California Institute of Technology, Division of Geological and Planetary Sciences Sessions, Alex; California Institute of Technology, Division of Geological and Planetary Sciences Adkins, Jess; California Institute of Technology, Division of Geological and Planetary Sciences Dalleska, Nathan; California Institute of Technology, Environmental Analysis Center Turchyn, Alexandra; University of Cambridge, Department of Earth Sciences Clegg, Josephine; University of Cambridge, Department of Earth Sciences Moradian, Annie; California Institute of Technology, Proteome Exploration Laboratory Sweredoski, Michael; California Institute of Technology, Proteome Exploration Laboratory Garbis, Spiros; California Institute of Technology, Proteome Exploration Laboratory Eiler, John; California Institute of Technology, Division of Geological and Planetary Sciences

Stable isotope analysis of intact oxyanions using electrospray Quadrupole-Orbitrap mass spectrometry

Cajetan Neubauer[1,*,‡], Antoine Crémière[1], Xingchen T. Wang[1], Nivedita Thiagarajan[1], Alex L. Sessions[1], Jess F. Adkins[1], Nathan F. Dalleska[2], Alexandra V. Turchyn[3], Josephine A. Clegg[3], Annie Moradian[4], Michael J. Sweredoski[4], Spiros D. Garbis[4], John M. Eiler[1]

1. Division of Geological and Planetary Sciences, California Institute of Technology, Pasadena, CA 91125, USA.

2. Environmental Analysis Center, California Institute of Technology, Pasadena, CA 91125, USA

3. Department of Earth Sciences, University of Cambridge, Cambridge, CB2 3EQ, United Kingdom.

4. Proteome Exploration Laboratory, California Institute of Technology, Pasadena, CA 91125, USA.

* Corresponding author: 123caj@gmail.com

‡ Present address: Hanse-Wissenschaftskolleg, Lehmkuhlenbusch 4, 22753 Delmenhorst, Germany

Running title: Sulfate and nitrate isotopic analyses using electrospray-Orbitrap-MS

Keywords: Sulfate, nitrate, Orbitrap, electrospray, isotopolog, isotopologue

Abstract

The stable isotopes of sulfate, nitrate, and phosphate are frequently used to study geobiological processes of the atmosphere, ocean, as well as land. Conventionally, the isotopes of these and other oxyanions are measured by isotope-ratio sector mass spectrometers after conversion into gases. Such methods are prone to various limitations on sensitivity, sample throughput, or precision. In addition, there is no general tool that can analyze several oxyanions or all the chemical elements they contain. Here, we describe a new approach that can potentially overcome some of these limitations based on electrospray hyphenated with Quadrupole Orbitrap mass spectrometry. This technique yields average accuracy of 1-2 ‰ for sulfate $\delta^{34}S$ and $\delta^{18}O$ and nitrate $\delta^{15}N$ and $\delta^{18}O$, based on in-house and international standards. Less abundant variants such as $\delta^{17}O$, $\delta^{33}S$ and $\delta^{36}S$ and the ^{34}S-^{18}O 'clumped' sulfate can be quantified simultaneously. The observed precision of isotope ratios is limited by the number of ions counted. The counting of rare ions can be accelerated by removing abundant ions with the quadrupole mass filter. Electrospray mass spectrometry (ESMS) exhibits high-throughput and sufficient sensitivity. For example, far less than 1 nmol sulfate is required to determine $^{18}O/^{34}S$ ratios with 0.2 ‰ precision within minutes. A purification step is recommended for environmental samples as our proposed technique is susceptible to matrix effects. Building upon these initial provisions, new features of the isotopic anatomy of mineral ions can now be explored with ESMS instruments that are increasingly available to bioanalytical laboratories.

Introduction

Oxyanions are important chemical constituents of virtually every environment on Earth, from ocean to groundwater to atmospheric aerosols. In biological organisms, oxyanions are both products and reactants in ecologically significant metabolic reactions. Additionally, the isotopic compositions of oxyanions are indispensable tools for studying biogeochemical cycles of sulfur and nitrogen, both today and in the past. For example, sulfate (SO_4^{2-}) is abundant in ocean waters and its isotopic composition reveals information about microbial sulfate reduction in anoxic seabeds (a major pathway for the remineralization of organic matter) and the role of sulfur oxidizing and reducing bacteria in oxygen-minimum zones (regions of the ocean that are inhospitable for higher organisms).[1,2] The isotopic composition of marine sulfate records is affected by changes in continental weathering, ocean chemistry and the injection of volcanic SO_2 into the atmosphere throughout Earth history.[3,4] Nitrate (NO_3^-) is the predominant form of bioavailable nitrogen in the ocean, and observations of its isotopes provide means of studying the nitrogen cycle, including N_2-fixation, nitrate assimilation, and denitrification.[5] Human activities have greatly altered the modern nitrogen cycle through fertilizer use and fossil fuel burning. A better understanding of the fate of anthropogenic nitrate in modern ecosystems through its isotopes is useful to mitigate the long-term impact of anthropogenic nitrogen on the safety of drinking water and the loss of biodiversity.[6] Studies of sulfate, nitrate and other ions such as phosphate could be advanced by methodological innovations that improve sensitivity, precision, the specificity of isotopic signatures, or sample throughput for the isotopic analysis of oxyanions.

Existing methods for analyzing the isotopic contents of oxyanions have limitations. Most established methods require the conversion of the sample ion into a room temperature gas (e.g., by combustion of sulfate into SO_2 or fluorination of sulfate to SF_6), which is then analyzed for its isotopic content by electron impact ionization followed by multi-collector (MC) sector mass spectrometry (Table S1). Alternatively, the sample oxyanions can be introduced to the ion source of an inductively

coupled plasma (ICP) isotope-ratio sector mass spectrometer, where it is dissociated and ionized prior to mass spectrometric analysis of the element of interest (this second method has been applied to S but not N).[7] These approaches do not permit simultaneous analysis of the isotopes of O and the other element in the oxyanion (i.e., S or N), meaning two separate measurements with different protocols would be required to obtain both independent pieces of information (but note that the denitrifier method [8] can measure $\delta^{15}N$ and $\delta^{18}O$ of nitrate using a single work-flow, while nitrate $\delta^{17}O$ analysis requires further thermal decomposition of N_2O to O_2). Moreover, existing techniques generally cannot be used to measure proportions of multiply-substituted isotopologs, such as $^{34}S^{18}O^{16}O_3^{2-}$ or $^{15}N^{18}O^{16}O_2^-$ (but see the recent effort [9] to measure ^{34}S-^{18}O clumping after partial fluorination of sulfate into SO_2F_2). More generally, all such methods that involve conversion to gases require chemical transformation and purification techniques that introduce added time, cost, and experimental bias, potentially limiting analytical precision and increasing sample size requirements.

Here we present a method for simultaneous measurement of multiple singly- and multiply-substituted isotopic forms of diverse oxyanions by a combination of electrospray (ES), a quadrupole mass filter and an Orbitrap mass analyzer. This work builds upon recent isotope-ratio measurements of intact biomolecules [10–12] and analysis of perchlorate.[13] We are not aware of any prior studies of the use of electrospray for precisely (approximately ±1 per mil) measuring natural-level isotope differences in oxyanions, perhaps because electrospray can be difficult to stabilize and advances in instrument design and signal processing were needed to overcome sources of noise or artifacts.[12,14] In mass spectrometric measurements that apply negative mode ES to identify organic compounds in complex mixtures, oxyanions are commonly observed as background ions.[15] Previous analyses of oxyanions by electrospray MS (ESMS) have mainly focused on the quantification of solute concentration, or studies of ion hydration, elemental speciation, tracer incorporation and self-oligomerization.[16–20]

The purpose of this study is to document the methods and performance characteristics of measurements of the isotopic composition of sulfate and nitrate by ESMS. This effort is motivated by the fact that the approach we present is capable of rapid, highly sensitive, simultaneous measurements of all singly- and multiply-substituted isotopic forms of such species, sometimes with minimal demands for sample preparation. The approach can be extended to other oxyanions that are amenable to electrospray ionization such as phosphate. Our results indicate that isotopologs of intact oxyanions can be detected at the natural abundance level by ESMS and quantified with precision down to 0.2 ‰ (with possibilities for further improvement).

Materials and Methods

Sulfate, nitrate and phosphate materials. Sodium sulfate (Na_2SO_4) was obtained from the Caltech mineral collection and commercial suppliers that produce Na_2SO_4 of natural and synthetic origin (Table S2). 100 mM stock solutions were prepared in LC/MS grade water (LiChrosolv 1.15333, EMD Millipore; sulfate or nitrate ≤10 ppb). The stock solutions were diluted to 50 μM in methanol (LiChrosolv 1.06035, EMD Millipore) or a 7:3 mixture of methanol and water. These working solutions were used for direct infusion. Potassium nitrate reference materials USGS32 and USGS34 were provided by the US Geological Service (USGS). 100 mM KNO_3 stock solutions were prepared in a 1:1 mixture of LC/MS grade water and methanol. The stock solutions were diluted to 50 μM in methanol. A 100 mM stock solution of potassium phosphate (KH_2PO_4, Mallinckrodt 7100-12) was prepared in water and diluted to 50 μM in methanol for direct infusion.

ESMS instrumentation, data collection, and analysis. A Q Exactive HF Orbitrap mass spectrometer (Thermo Fisher Scientific) was coupled to a digitally controlled syringe pump (Fusion 101, Chemyx) that delivered oxyanion solutions at a flow rate of 1 μl/min from a syringe (Model # 81265, Hamilton Robotics) to an Ion Max API electrospray ion source, which was connected to a HESI-II probe (Thermo

Fisher Scientific). The following ionization settings were used: sheath gas flow rate: 0, auxiliary gas flow rate: 0, sweep gas flow rate: 0, spray voltage: 3.0 kV, spray current (observed): 0.2 µA, capillary temperature: 320 °C, S-lens RF level: 60, auxiliary gas heater temp (actual): 35-40 °C.

Mass spectrometer data were collected in negative ionization mode, using the following settings for sulfate as default: scan type: selected ion monitoring (SIM); scan range (isolation range): *m/z* 87–107; fragmentation: none; resolution: R = 30,000 or R = 60,000 (throughout the text R refers to the Orbitrap resolution setting, which equals the mass resolving power (FWHM) at *m/z* 200; actual mass resolving power was generally higher, by a factor of $[200/(m/z)]^{0.5}$); polarity: negative; microscans: 1; lock masses: off; AGC target: 300,000; AGC prescan mode: -1; maximum injection time: 500 ms. For the selection of isotopologs (overview without monoisotopic peak), an Orbitrap scan range and quadrupole isolation range of *m/z* 97–107 was used. Profile mode data was collected using the Q Exactive HF Tune software (instrument version 2.8 Build 280502, software version 2.8 SP1 Build 2806). For nitrate and phosphate samples the same settings were used, except the scan range was set to *m/z* 60–66 (nitrate) or *m/z* 87–107 (phosphate); resolution: R = 15,000 or R = 30,000 (nitrate), R = 120,000 (phosphate).

The software FTStatistic (Thermo Fisher Scientific) was used for the extraction of ion intensities from RAW files.[12] R (version 3.5.1), RStudio, and the R-packages dplyr, tidyr, and ggplot2 were used for data analysis.

Calculation of delta values from ESMS data. Sulfate isotopic composition was calculated relative to an in-house reference ('Chaplin' sample; Table S2): $\delta^{18}O_{HSO4} = \frac{({}^{1}H^{32}S^{18}O^{16}O_3/{}^{1}H^{32}S^{16}O_4)_{sample}}{({}^{1}H^{32}S^{18}O^{16}O_3/{}^{1}H^{32}S^{16}O_4)_{reference}} - 1$; $\delta^{34}S_{HSO4} = \frac{({}^{1}H^{34}S^{16}O_4/{}^{1}H^{32}S^{16}O_4)_{sample}}{({}^{1}H^{34}S^{16}O_4/{}^{1}H^{32}S^{16}O_4)_{reference}} - 1$. Nitrate isotopic composition was calculated relative to the

USGS32 reference material: $\delta^{18}O_{NO3} = \frac{(^{14}N^{18}O^{16}O_2/^{14}N^{16}O_3)_{sample}}{(^{14}N^{18}O^{16}O_2/^{14}N^{16}O_3)_{reference}} - 1$; $\delta^{15}N_{NO3} = \frac{(^{15}N^{16}O_3/^{14}N^{16}O_3)_{sample}}{(^{15}N^{16}O_3/^{14}N^{16}O_3)_{reference}} - 1$

.

Bulk isotopic composition. The $\delta^{34}S_{SO4}$ and $\delta^{18}O_{SO4}$ values of in-house reference standards were obtained by conventional IRMS methods (see Supporting Information). The isotopic composition of sulfate and nitrate materials are summarized in Table S2.

Predicted sulfate isotopolog ratios. Based on measured $\delta^{34}S_{SO4}$ and $\delta^{18}O_{SO4}$ values, ^{33}S ($^{33}\lambda$=0.515), ^{36}S ($^{36}\lambda$=1.89) and ^{17}O ($^{17}\lambda$=0.52) abundances were inferred, using the equations for mass-dependent fractionation $^{3x}\lambda = ln(1 + \delta^{3x}S)/ln(1 + \delta^{34}S)$ and $^{17}\lambda = ln(1 + \delta^{17}O)/ln(1 + \delta^{18}O)$. Isotope abundances were then used to calculate the stochastic occurrence of $^{34}S^{18}O_{HSO4}$ and $^{36}S_{HSO4}$. VCDT reference was assumed to contain 94.93% ^{32}S, 4.29% ^{34}S, 0.76% ^{33}S, and 0.02% ^{36}S. For VSMOW, $^{18}O/^{16}O$ ratios of 2005.20 ppm and $^{17}O/^{16}O$ of 379.9 ppm were assumed.

Results and Discussion

Observable isotopologs

The main benefit of soft ionization is that a diverse set of isotopologs can be observed simultaneously as soon as intact ions can be ionized and transferred into the mass spectrometer. We first established suitable electrospray conditions. Current Orbitrap MS instruments do not transmit ions below *m/z* 50; therefore ions with a smaller *m/z* cannot be detected. For example, this rules out the analysis of SO_4^{2-} at *m/z* 48 (n.b., this ion is likely unstable in the gas phase).[18] The singly-charged oxyanions HSO_4^-, $H_2PO_4^-$ and NO_3^- are all above this mass cut-off and detectable, yet their signal intensity is unstable under many ionization conditions. Sulfate ions are also prone to form a salt precipitate, which blocks the electrospray in the presence of certain counter ions such as barium. In addition, we found that pH modifiers will compete with oxyanions for ionization and hence decrease their ionization efficiency. Therefore, we

dissolved low concentrations (μmol/L) of sulfate, nitrate and phosphate salts in otherwise pure methanol-water mixtures. Contrary to our initial expectation, stable ionization of the singly-charged oxyanions was achieved by direct infusion with relatively low flow rates (~1 μL/min) and using low proportion or no added water. No major alternative ionization species such as dehydrated ions (e.g., SO_3^-), adducts or clusters were observed. These ionization tests yielded a procedure by which diverse oxyanions can be efficiently ionized by electrospray and transferred into the MS.

At a moderate resolution (R = 30,000), the Orbitrap resolves the main A+1 and A+2 isotopologs of HSO_4^- from one another (Fig. 1). Specifically, $^1H^{33}S^{16}O_4^-$ is resolved from $^1H^{32}S^{17}O^{16}O_3^-$, and $^1H^{34}S^{16}O_4^-$ is resolved from $^1H^{32}S^{18}O^{16}O_3^-$ (for better readability, isotopologs of HSO_4^- are stated in the remaining text by their main substitution, e.g. $^{18}O_{HSO4}$ is identical to $^1H^{32}S^{18}O^{16}O_3^-$). These four isotopologs together with the monoisotopic peak ($^1H^{32}S^{16}O_4^-$, the 'base peak') represent almost all of the HSO_4^- ions (>99.9 %). Additional rare variants require careful adjustments to ensure detection in every scan. For instance, $^2H_{HSO4}$ can be resolved at higher resolution; the signals of the A+4 isotopologs, containing $^{36}S_{HSO4}$ or $^{34}S^{18}O_{HSO4}$, benefit from using a narrower mass window to increase their relative abundance (e.g., *m/z* 97–107). Certain rare isotopologs are not resolvable. In the most notable case, $^{18}O_{HSO4}$ and $^{33}S^{17}O_{HSO4}$ differ by only 0.6 mDa and are not resolved. $^{33}S^{17}O_{HSO4}$ is 500-fold less abundant than $^{18}O_{HSO4}$ (>42,000 parts per million; no attempts were made in subsequent signal processing to correct for the contribution of $^{33}S^{17}O_{HSO4}$). Other A+2 isotopologs would be readily resolvable but are not detected because they are very rare (e.g., $^{17}O^{17}O_{HSO4}$ <1 ppm). Overall, the ESMS spectra of sulfate contain potentially useful and novel isotopic information, in particular, the resolved peaks contain information about S and O isotopic content in a single measurement.

When choosing the Orbitrap resolution, the impact of rare and/or unresolved species on isotopolog ratios has to be considered. The choice of resolution has trade-offs. Sufficient resolution is required to resolve all major isotopologs. Furthermore, acquiring scans at high resolution is convenient

to ensure that isotope data is not contaminated by other chemical species (e.g., HSO_4^- and $H_2PO_4^-$ both have nominal mass 97). Yet, using lower resolution also has advantages. Firstly, the scan time ('transient length') of the Orbitrap increases proportionally with increasing resolution. Together with the fact that ion accumulation in the C-trap represents a larger proportion of the transient length at a lower resolution, this means that twice the number of ions can be counted when half the nominal resolution is used. Secondly, a by-product of the shorter scan time is a more robust signal, because fewer ions are lost during the detection due to unstable flight paths in the Orbitrap (n.b., ion signal decays over time in the Orbitrap). In the case of nitrate, a lower resolution (R = 15,000) is sufficient to resolve $^{15}N_{NO3}$, $^{17}O_{NO3}$, and $^{18}O_{NO3}$, whereas for phosphate ($H_2PO_4^-$) a higher resolution may be useful to resolve the relatively abundant $^{2}H_{H2PO4}$ (Fig. 1). Thus, for different analytes and aims the most appropriate resolution setting can be selected.

Precision

We have previously reported that ratios of isotopologs in fragment ions of the amino acid methionine can be measured with experimental precision limited by counting statistics (i.e., depends predictably on how many ions have been counted) by ESMS, down to levels of ±0.03 ‰ (1 RSE; "isotope barcoding" procedure).[10] In the present study, we examined whether ion intensity ratios of isotopologs of oxyanions also can be measured with precision near shot-noise limits when the analyte is delivered to the ES source by continuous direct infusion using a syringe pump. We found that the analytical precision of the isotope ratios is also limited by how many ions have been counted (Fig. 1). Specifically, a 15 minute period of continuous acquisition yields a measurement of the ratio $^{34}S_{HSO4}/^{1}H^{32}S^{16}O_4^-$ with an external error of 0.23 ‰ (1 RSE; shot-noise limit 0.18 ‰; AGC 3E5). Ion intensity ratios involving less abundant isotopic forms have a proportionally poorer external error in the same acquisition (0.5‰ for $^{33}S_{HSO4}$ and $^{18}O_{HSO4}$ (limit 0.4 ‰); 1.5 ‰ for $^{17}O_{HSO4}$ (limit 1.0 ‰)). These observations indicate that the analytical precision of measurements by ESMS allows the detection of isotope variations at the

sub-permil level. The analytical precision depends on how many ions have been counted (at least on the timescale of minutes to tens of minutes).

Accuracy

High accuracy is required for the study of naturally-occurring isotope fractionations. In order to assess the accuracy of the ESMS method, we obtained sulfate and nitrate samples and characterized them for their isotopic contents using methods with well-established accuracy. Throughout, we use the conventional δ notation for isotope ratios, e.g. $\delta^{34}S = (\frac{(^{34}S/^{32}S)_{sample}}{(^{34}S/^{32}S)_{reference}} - 1)$, but for ratios measured by ESMS data we replace isotopes with isotopologs; e.g., $\delta^{34}S_{HSO4} = \frac{(^{1}H^{34}S^{16}O_4/^{1}H^{32}S^{16}O_4)_{sample}}{(^{1}H^{34}S^{16}O_4/^{1}H^{32}S^{16}O_4)_{reference}} - 1$.

Sulfate

There are currently no sulfate standards with certified (by IUPAC) $\delta^{34}S$, $\delta^{33}S$, and $\delta^{18}O$ values for comparison with ESMS measurements. In order to estimate the accuracy of the ESMS method, we first characterize sulfate materials that are suitable for comparison with IRMS methods that independently yield sulfate $\delta^{18}O$ and $\delta^{34}S$ ($\delta^{18}O$: pyrolysis to form CO; $\delta^{34}S$: combustion into SO_2). Sodium sulfate was selected as the form of our sulfate accuracy standards because it has a high solubility in water, can be analyzed by electrospray and IRMS (for $\delta^{18}O$ after precipitation by titration with $BaCl_2$ – see Supporting Information) and is available in nearly pure form from globally distributed mining operations, geological deposits, and industrial production. We obtained nine sulfates and measured their S and O isotope contents separately by gas source IRMS (Table S2). The results indicate that these sulfates span a substantial range of $\delta^{34}S_{SO4}$ (-10 to +21 ‰$_{VCDT}$) and $\delta^{18}O_{SO4}$ values (+8 to +20 ‰$_{VSMOW}$). The two isotope dimensions are only weakly correlated with one another (Pearson's coefficient r = 0.31), and several sample pairs are similar in one isotopic dimension yet differ in the other. For example, Cedar Lake and Soda Lake sulfate have similar $\delta^{18}O_{SO4}$ but their $\delta^{34}S_{SO4}$ differs by 21 ‰$_{VCDT}$.

We analyzed the sodium sulfates for their ratios of $^{34}S/^{32}S$ and $^{18}O/^{16}O$ by ESMS and compared their apparent differences in $\delta^{34}S$ and $\delta^{18}O$ with values observed by TC/EA. The ESMS values of $\delta^{34}S_{HSO4}$ and $\delta^{18}O_{HSO4}$ (normalized to sample 'Chaplin', which we assigned as an internal standard) are correlated with the $\delta^{34}S_{SO4}$ and $\delta^{18}O_{SO4}$ values obtained by TC/EA (Fig. 2; Pearson's coefficient r = 0.998 for ^{34}S, r = 0.990 for ^{18}O). ESMS yielded on average slightly higher $\delta^{34}S_{HSO4}$ values (+0.7 ‰). The mean absolute difference from the true $\delta^{34}S_{SO4}$ values was 0.8 ‰ (SD = 0.5 ‰). One sample (Trona) was measured five times by ESMS. These repeat analyses had a somewhat higher variability of $\delta^{34}S_{HSO4}$ (SD = 1.8 ‰). Overall, the ^{34}S data closely conform to a 1:1 proportionality between isotopic differences between sulfate materials measured by these two techniques. Together, these tests indicate that $\delta^{34}S_{HSO4}$ was determined with an accuracy of 1-2 ‰; without applying procedures that can further improve accuracy, such as bracketing of samples in between runs of the reference and applying a correction factor for drift of the signals.

The regression comparing expected and measured $\delta^{18}O$ values showed a linear relationship, but with an increased slope of 1.17 (Fig 2). The difference of ^{34}S content of in the sulfate materials should not affect the slope ($\delta^{34}S_{SO4}$ range: 30 $‰_{VCDT}$). Rather, the comparison for the $^{18}O/^{16}O$ ratios from the two techniques is less constrained than for sulfur because the O isotopic contents in the reference set span a smaller range and were determined by TC/EA with a lower precision ($\delta^{18}O_{SO4}$ range: 11 ‰; precision was 0.2 % for $\delta^{34}S_{SO4}$ and 0.7 ‰ for $\delta^{18}O_{SO4}$). The sulfate material from Trona, which has the highest $\delta^{18}O_{SO4}$, strongly affects the slope of the regression. It was measured in five replicates, one of which may be an outlier. If this individual data point is removed, the slope of the regression is close to 1 (1.04). Together, these comparisons of ESMS and TC/EA data for sulfate materials suggest that $\delta^{34}S$ and $\delta^{18}O$ values were measured by ESMS with an accuracy of about 1-2 ‰ (relative to an in-house standard). This level of accuracy may be useful for environmental questions, for example when it is beneficial to measure S and O isotopes during microbial S cycling. The comparison also provides a basis for

improved experimental design, reference materials and data analysis. All of these have the potential to optimize accuracy and sensitivity for sulfate isotopic measurements.

Nitrate

We used ESMS to measure the N and O isotopic content of two available potassium nitrate reference materials (Fig. 2). The $\delta^{15}N$ of the USGS32 and USGS34 standards have an independently known difference of 182.1 $‰_{air}$, and a difference measured by ESMS of 175.2±1.6‰, suggesting a subtle compression of the scale of isotopic variations as measured by ESMS. We tested whether the scale compression is consistent across the range of composition by preparing a 1:1 mixture of USGS 32 and 34. The measured $\delta^{15}N_{NO3}$ of this mixture showed a linear response (R^2 >0.99). A close match was also observed for $\delta^{18}O$ (expected: 54.9 $‰_{VSMOW}$, measured: 53.9±1.2 ‰). These tests with nitrate indicate that ESMS can achieve levels of accuracy needed for environmental applications.

Together, these tests with sulfate and nitrate demonstrate that ESMS can have sufficient accuracy to be useful to study natural differences of the stable isotope contents of mineral ions. Relatively rare isotopologs such as the $^{17}O_{HSO4}$ (abundance < 0.2%) could be quantified but may require slight adjustments to data collection, processing, and validation.

Rare singly-substituted isotopologs

Rare ions (e.g., isotopologs $^{17}O_{HSO4}$, $^{33}S_{HSO4}$, $^{36}S_{HSO4}$) are of interest for applications that quantify mass-independent isotope fractionation, which for example can be caused by photochemical reactions of sulfur in the atmosphere.[21] However, the counting of rare isotopologs is time-consuming when analyzing the entire ion population because each Orbitrap scan has a limit of how many ions can be analyzed without causing artifacts (e.g., ion coalescence). A raw comparison of the isotopolog abundances puts this limitation into perspective: if it took 1 minute to count 1 million ions of the singly-substituted

$^{34}S_{HSO4}$ isotopolog, it would take about 6 minutes to count the same number of $^{18}O_{HSO4}$ or $^{33}S_{HSO4}$. Even much longer experiment would be required to achieve a comparable counts/precision for $^{17}O_{HSO4}$ (>30 min), $^{36}S_{HSO4}$ (>2,000 min) or the $^{34}S^{18}O_{HSO4}$ clumped isotopolog (>200 min).

Therefore, we tested whether rare ions can be counted more efficiently by removing abundant isotopologs using the quadrupole. For example, using a mass range of *m/z* 97–107 largely eliminates the monoisotopic peak of HSO_4^- (*m/z* 96.960), which represents 94 % of the HSO_4^- ions. In this way, sulfate ions that contain one or more rare isotopes become enriched and can be counted more quickly. At this quadrupole setting, we can measure the intensity ratios of the $^{18}O_{HSO4}$, $^{17}O_{HSO4}$, $^{33}S_{HSO4}$ and $^{36}S_{HSO4}$ versus $^{34}S_{HSO4}$ with relative external errors of 0.2, 0.5, 0.2 and 1.2‰, respectively in 15 minutes (R = 30,000; 14 scans/s; AGC 3E5). Compared to ESMS analysis using a mass range that includes the monoisotopic peak, this represents an improvement in time efficiency of about one order of magnitude. For example, it took 2 minutes instead of 18 minutes to count 1 million ions of the ^{17}O isotopolog once the base peak was eliminated. The observed speed up is lower than theoretically expected because ion transmission through the quadrupole decreases when isolating a smaller *m/z* range. As the ion transmission function of a quadrupole is not an ideal rectangular step function, ratios of isotopologs that have the same nominal mass (e.g., $^{18}O_{HSO4}/^{34}S_{HSO4}$) are expected to yield the most accurate isotope ratios when using the elimination of the monoisotopic ions. In sum, we find that the exclusion of the monoisotopic peak is a time-efficient strategy to quantify rare isotopologs.

For sulfate of most origins, the isotopes of the same element (i.e., the three O isotopes or the four S isotopes) are expected to vary in synchrony due to mass-dependent fractionation. In order to assess whether ESMS yields isotope ratios that vary according to mass-dependent fractionation, we measured the three sulfate materials with the largest differences in ^{34}S and ^{18}O contents (Trona, Antarctica, Soda Lake) by excluding the monoisotopic peak. The ion counts for $^{33}S_{HSO4}$, $^{34}S_{HSO4}$, and $^{36}S_{HSO4}$, as well as $^{17}O_{HSO4}$ and $^{18}O_{HSO4}$ are consistent with a linear relationship (R^2 >0.99; Fig. 3A). This

suggests that excluding the base peak does not cause obvious changes to the predicted near-linear relationship between these rare isotopes. Future work is required to address the apparent accuracy of multiple isotope measurements and whether the strategy outlined here can be refined to quantify mass-independent isotope effects.

Rare doubly-substituted isotopologs

'Isotope clumping' refers to the phenomenon that heavier isotopes are often thermodynamically more likely to bind to other heavy isotopes than one would expect by random chance. The extent to which isotope clumps occur depends in part on the temperature at the time of formation. This temperature relation has facilitated the development of clumped isotope 'thermometers' based on the isotopic content of gases, e.g. CO_2 and methane.[22] It is conceivable that clumped isotopes of oxyanions (sulfate, borate, perchlorate, and others) may also encode useful information, but no established methods exist to observe such isotopic species.

When we perform an ESMS experiment on sulfate that eliminates the base peak by pre-filtering the mass spectrum using the quadrupole, a ratio involving a clumped isotope species ($^{34}S^{18}O_{HSO4}$/ $^{34}S_{HSO4}$) can be measured with relative external standard error of 0.7 ‰ (15 min., *m/z* 97–107*,* AGC 3E5). Ion counting can be accelerated further, by using a narrow quadrupole window to select only A+4 ions (*m/z* 101±0.5). Measurement of this narrow mass window allows us to measure the ion intensity ratio, $^{34}S^{18}O_{HSO4}$/ $^{36}S_{HSO4}$ with a relative external error of 0.5 ‰ within 15 minutes. In practice, however, ratios measured via the second method had poor reproducibility. This failure to replicate may in part be caused by the lower and more variable ion transmission in the quadrupole when using a narrow mass selection window. Thus, eliminating the base peak (but not filtering the A+4 ions) appears to be the better strategy to measure clumped isotopes at this time.

To a first order, the signal intensity of $^{34}S^{18}O_{HSO4}$ will depend on the ^{18}O and ^{34}S content of the sample. Based on the independently measured $\delta^{18}O_{SO4}$ and $\delta^{34}S_{SO4}$, we predict that the Antarctica sample

should have the lowest, Trona the second lowest and Soda Lake the highest $\frac{^{34}S^{18}O_{HSO4}}{^{36}S_{HSO4}}$ ratio (for calculations see Methods; we use $^{36}S_{HSO4}$ as denominator because it is near-isobaric with $^{34}S^{18}O_{HSO4}$). This expected order is confirmed by the ESMS measurement (Fig. 3B). However, 'isotope clumping' has to be measured relative to the expected stochastic occurrence of $^{34}S^{18}O_{HSO4}$. As we do not have samples measured with a stochastic distribution of $^{34}S^{18}O_{HSO4}$, we instead define a reference line between the average of Trona (our most precisely measured sample) and the origin. Δ_{34S18O}, defined here as the difference between the measured $\frac{^{34}S^{18}O_{HSO4}}{^{36}S_{HSO4}}$ and the extrapolated reference value (black line in Fig. 3B), indicate that the samples Soda Lake and Trona have a higher $^{34}S^{18}O$-clumping than Antarctica sulfate.

These initial tests indicate that ESMS appears to provide a path towards measuring isotope clumping using the intact sulfate molecule. $^{34}S^{18}O_{HSO4}$ should now be measured on sulfate materials that have been produced under known and controlled conditions. A comparison of samples with an emerging IRMS method based on partial fluorination for sulfate into SO_2F_2 may be particularly suited for method development and to determine whether isotope clumping on sulfate could be developed as a geochemical tool.[9] Potential applications of this clumped isotope sulfate would be as a paleothermometer or to obtain additional constraints in the role of enhanced sulfide oxidation on riverine and seawater sulfate.

Sensitivity

In retrospect, it is obvious that oxyanions can be efficiently transferred into the mass spectrometer by electrospray because they already exist as anions in solution. This poses the question of whether ESMS can be more sensitive than established methods, which require nanomole or micromole amounts of sulfate or nitrate (Table S2). We find that sulfate, nitrate, and phosphate all require similar electrospray conditions and have equivalent ion yields. The ionization is most efficient when low flow rates and high content of organic solvents are used. A typical direct infusion experiment of sodium sulfate requires <1

nmol to constrain the $^{18}O_{HSO4}/^{34}S_{HSO4}$ ratio to 0.2 ‰ (50 µM in methanol, flow 1 µL/min, 15 min., *m/z* 97–107). We find that this sample amount can be lowered by an order of magnitude by decreasing the concentration, without altering the isotope ratios. It is also possible to measure even lower sample concentrations (e.g., 1 µmol/L), however, at such low concentrations, the ion accumulation time in the C-trap increases, to compensate for the loss of signal. This consequently decreases the speed of data acquisition. Furthermore, contaminating background, including ambient sulfate, make up a larger proportion of the analyzed ion population. Because sulfate and nitrate are common in most laboratory environments (background levels in our setup were up to ~1 µmol/L), analyzing samples at very low dilutions may not be appropriate. Overall, our results indicate that measuring oxyanions by electrospray is very sensitive. The tests indicate that ESMS may provide a path to decrease sample requirements for isotope analysis of oxyanions into the picomolar range.

There remains room for considerable improvement in the sensitivity of the ESMS method. For example, it often takes much longer for the Orbitrap to finish one scan than to collect ions for the next scan. This means that even at relatively low sulfate concentration, most of the HSO_4^- ions that have entered the mass spectrometer are lost to the vacuum (at 50 µM, only 0.5-15% of the ions are utilized; 5 µM: 3-50%). The utilization of ions could be enhanced by using nanoelectrospray and counting more ions per Orbitrap scan (however, artifacts in the Orbitrap can occur at high AGC settings, e.g. ‘ion coalescence’). The high sensitivity of ESMS suggests that with automated sample injection and optimized utilization of oxyanions by the mass analyzer, typical sample requirements could be in the low picomole range.

Conclusions

Our findings emphasize that there is a substantial, untapped potential for measuring the stable isotope contents of intact oxyanions. The observed accuracy, sensitivity, and the larger diversity of isotopologs

observed highlight that ESMS has unique features that motivate further refinement of the basic measurement principle outlined here. ESMS may not be limited to sulfate, nitrate or phosphate, but also provide paths towards analyzing the isotope contents of other oxyanions (e.g., arsenate, borate and perchlorate) and biological molecules (e.g. small organic acids) or chemical products that contain oxyanions, that can be released by MS/MS (e.g., phytate, nucleotides, glyphosate).

This study was designed as a coarse-grained survey of how oxyanion isotopes can be measured by ESMS and as such also identified focus areas for future method development. Most importantly, ESMS has different, often more stringent requirements for sample purity than established workflows. From initial tests of environmental water samples, it seems unlikely that simple dilute-and-shoot procedures will be applicable for complex sample types such as seawater. A combination of sample cleanup (e.g., affinity, ion exchange, precipitation) and dilution may enable routine isotope measurements by ESMS.

Supporting Information

Overview of existing methods for sulfate and nitrate isotopic analysis (Table S1). Details of the sulfate and nitrate materials used in this study (Table S2), including their isotopic composition. Description of methods used for determining bulk isotopic composition.

Acknowledgments

We thank the reviewers for comments. We are grateful for assistance provided by Roxana Eggleston-Rangel and Brett Lomenick, and thank George Rossmann as well as the companies Peñoles, Crimidesa, Saltex, Airborne Industrial Minerals, and Searles Valley Minerals for providing sulfates. This study was using ESMS instrumentation at the Proteome Exploration Laboratory (supported by Beckman Institute, and NIH 1S10OD02001301). CN is a fellow of the Hanse-Wissenschaftskolleg.

References

(1) Jørgensen, B. B.; Findlay, A. J.; Pellerin, A. The Biogeochemical Sulfur Cycle of Marine Sediments. *Front. Microbiol.* **2019**, *10*, 849.

(2) Canfield, D. E.; Stewart, F. J.; Thamdrup, B.; De Brabandere, L.; Dalsgaard, T.; Delong, E. F.; Revsbech, N. P.; Ulloa, O. A Cryptic Sulfur Cycle in Oxygen-Minimum–Zone Waters off the Chilean Coast. *Science* **2010**, *330* (6009), 1375–1378.

(3) Claypool, G. E.; Holser, W. T.; Kaplan, I. R.; Sakai, H.; Zak, I. The Age Curves of Sulfur and Oxygen Isotopes in Marine Sulfate and Their Mutual Interpretation. *Chem. Geol.* **1980**, *28*, 199–260.

(4) Paytan, A.; Kastner, M.; Campbell, D.; Thiemens, M. H. Sulfur Isotopic Composition of Cenozoic Seawater Sulfate. *Science* **1998**, *282* (5393), 1459–1462.

(5) Sigman, D. M.; Fripiat, F. Nitrogen Isotopes in the Ocean. *Encyclopedia of Ocean Sciences*. 2019, pp 263–278.

(6) OECD. *Human Acceleration of the Nitrogen Cycle: Managing Risks and Uncertainty*; OECD Publishing, https://doi.org/10.1787/9789264307438-en.

(7) Paris, G.; Sessions, A. L.; Subhas, A. V.; Adkins, J. F. MC-ICP-MS Measurement of $\delta^{34}S$ and $\Delta^{33}S$ in Small Amounts of Dissolved Sulfate. *Chemical Geology*. 2013, pp 50–61.

(8) Sigman, D. M.; Casciotti, K. L.; Andreani, M.; Barford, C.; Galanter, M.; Böhlke, J. K. A Bacterial Method for the Nitrogen Isotopic Analysis of Nitrate in Seawater and Freshwater. *Anal. Chem.* **2001**, *73* (17), 4145–4153.

(9) Ueno, Y.; Katsuta, T.; Ishimaru, T.; Yoshida, N. A New Method for Measuring ^{34}S-^{18}O Clumping of Sulfate. In *Goldschmidt Conference Abstracts*; 2019.

(10) Neubauer, C.; Sweredoski, M. J.; Moradian, A.; Newman, D. K.; Robins, R. J.; Eiler, J. M. Scanning the Isotopic Structure of Molecules by Tandem Mass Spectrometry. *Int. J. Mass Spectrom.* **2018**, *434*, 276–286.

(11) Neubauer, C.; Sessions, A. L.; Booth, I. R.; Bowen, B. P.; Kopf, S. H.; Newman, D. K.; Dalleska, N. F. Towards Measuring Growth Rates of Pathogens during Infections by D_2O-Labeling Lipidomics. *Rapid Commun. Mass Spectrom.* **2018**, *32* (24), 2129–2140.

(12) Eiler, J.; Cesar, J.; Chimiak, L.; Dallas, B.; Grice, K.; Griep-Raming, J.; Juchelka, D.; Kitchen, N.; Lloyd, M.; Makarov, A.; et al. Analysis of Molecular Isotopic Structures at High Precision and Accuracy by Orbitrap Mass Spectrometry. *Int. J. Mass Spectrom.* **2017**, *422*, 126–142.

(13) Martin, P. E.; Farley, K. A.; Eiler, J. M. A New Method of Isotopic Analysis of Perchlorate Using Electrospray-Orbitrap Mass Spectrometry. In *GSA Annual Meeting in Indianapolis, Indiana, USA - 2018*; GSA, 2018; p Paper No. 124–11.

(14) Makarov, A.; Grinfeld, D.; Ayzikov, K. Fundamentals of Orbitrap Analyzer. In *Fundamentals and Applications of Fourier Transform Mass Spectrometry*; Kanawati, B., Schmitt-Kopplin, P., Eds.; books.google.com, 2019; Vol. Fundamentals of Orbitrap analyzer, pp 37–61.

(15) Keller, B. O.; Sui, J.; Young, A. B.; Whittal, R. M. Interferences and Contaminants Encountered in Modern Mass Spectrometry. *Anal. Chim. Acta* **2008**, *627* (1), 71–81.

(16) Safian, M. F.; Lehmann, W. D. Microquantification of Inorganic and Organic Phosphate by Negative Ion Electrospray Tandem Mass Spectrometry. *Anal. Bioanal. Chem.* **2015**, *407* (10), 2933–2937.

(17) Boismenu, D.; Robitaille, L.; Hamadeh, M. J.; Hongsprabhas, P.; Hoffer, L. J.; Mamer, O. A. Measurement of Sulfate Concentrations and Tracer/tracee Ratios in Biological Fluids by Electrospray Tandem Mass Spectrometry. *Anal. Biochem.* **1998**, *261* (1), 93–99.

(18) Blades, A. T.; Kebarle, P. Study of the Stability and Hydration of Doubly Charged Ions in the Gas Phase: SO_4^{2-}, $S_2O_6^{2-}$, $S_2O_8^{2-}$, and Some Related Species. *J. Am. Chem. Soc.* **1994**, *116* (23), 10761–10766.

(19) Agnes, G. R.; Stewart, I. I.; Horlick, G. Elemental Speciation Measurements with Electrospray Mass Spectrometry: An Assessment. *Appl. Spectrosc., AS* **1994**, *48* (11), 1347–1359.

(20) Gaspar, A.; Harir, M.; Lucio, M.; Hertkorn, N.; Schmitt-Kopplin, P. Targeted Borate Complex Formation as Followed with Electrospray Ionization Fourier Transform Ion Cyclotron Mass Spectrometry: Monomolecular Model System and Polyborate Formation. *Rapid Communications in Mass Spectrometry*. 2008, pp 3119–3129.

(21) Ono, S. Photochemistry of Sulfur Dioxide and the Origin of Mass-Independent Isotope Fractionation in Earth's Atmosphere. *Annu. Rev. Earth Planet. Sci.* **2017**, *45* (1), 301–329.

(22) Eiler, J. M. The Isotopic Anatomies of Molecules and Minerals. *Annu. Rev. Earth Planet. Sci.* **2013**, *41* (1), 411–441.

(23) John, S. G.; Adkins, J. F. Analysis of Dissolved Iron Isotopes in Seawater. *Mar. Chem.* **2010**, *119* (1), 65–76.

Figure Legends

Fig. 1 Mass spectra and precision of isotope ratios. (A) Representative mass spectra of sulfate (HSO_4^-), nitrate (NO_3^-) and phosphate ions ($H_2PO_4^-$). The mass regions corresponding to A+1 (green), A+2 (blue) are magnified. Data for the low-abundance sulfate A+4 ions were collected by removing the base peak ($^1H^{32}S^{16}O_4^-$) using the quadrupole. (B) Ratio of the sulfate $^{34}S_{HSO4}$ isotopolog versus the base peak from a representative data collection (R = 30,000; 14 scans/s; AGC 3E5). The light green line represents the mean of a moving window of 1 min. The distribution of isotopolog ratios is symmetric and its geometric mean (0.04859; black diamond plus) can be determined with high precision (relative standard error (RSE) 1σ = 0.23 ‰; y-axis is magnified to better show the error bars in red). (C) The RSE of isotope ratios is approximately limited by counting statistics. The log-log plot shows the RSE (1σ) of the measurement of the $^{34}S_{HSO4}$ isotopolog versus the HSO_4^- base peak plotted against the effective number of counted ions.[23] For isotopologs *a* and *b* the number of effective counts $n_{eff} = \frac{n_a \cdot n_b}{n_a + n_b}$. The blue line represents the shot-noise limit, $\sigma_{shot\ noise} = \sqrt{\frac{1}{n_{eff}}}$.

Fig. 2 Comparison of ESMS measurements with established IRMS methods. (A) Sulfate $\delta^{34}S$ from ESMS and combustion are highly correlated (Pearson's r > 0.994). The linear regression (blue) of the mean values has a slope close to 1 (95% confidence interval in grey). A dotted black line with slope = 1 is shown for comparison. Five independently measured data points for the Trona sample are shown as pink dots. Delta values are relative to sulfate from Chaplin, Canada (Table S2). (B) Sulfate $\delta^{18}O$ from ESMS and combustion are highly correlated (Pearson's r > 0.990). The linear regression has an increased slope when all replicates of the Trona sample (pink dots) are included in the analysis (slope 1.04, without potential outlier). Note that the confidence interval (grey) does not include uncertainty

associated with the expected δ value. (C) Nitrate $\delta^{15}N$ and (D) nitrate $\delta^{18}O$ measured by ESMS are highly correlated with independently known values for reference materials USGS32 and USGS34 and a 1:1 mixture of the two (Pearson's r = 0.999). Absolute $\delta^{18}O$ and $\delta^{15}N$ values from ESMS matched closely to the expected values. The isotopic difference was robustly detected also at a higher resolution (R = 30,000; green).

Fig. 3 Rare isotopologs of sulfate can be quantified with improved counting statistics by eliminating the base peak. (A) The ion counts per scan for $^{33}S_{HSO4}$, $^{34}S_{HSO4}$, and $^{36}S_{HSO4}$, as well as $^{17}O_{HSO4}$ and $^{18}O_{HSO4}$ are consistent with a near-linear relationship (R^2 >0.99), as expected for mass-dependent fractionation. (B) The signal of the clumped isotopolog $^{34}S^{18}O_{HSO4}$ varies between the tested sulfate materials. The black line represents a line of constant isotopic fractionation ($\alpha_{meas.-pred.} = \frac{R_{meas.}}{R_{pred.}}$; y-intercept = 0), defined by the average value of the Trona sample, which was measured at the beginning and end of data collection. Δ_{34S18O}, the difference between the measured $^{34}S^{18}O_{HSO4}$ / $^{36}S_{HSO4}$ and the extrapolated reference (black line), appears to indicate that the samples Soda Lake and Trona have a higher $^{34}S^{18}O$-clumping than Antarctica sulfate.

For Table of Contents Only

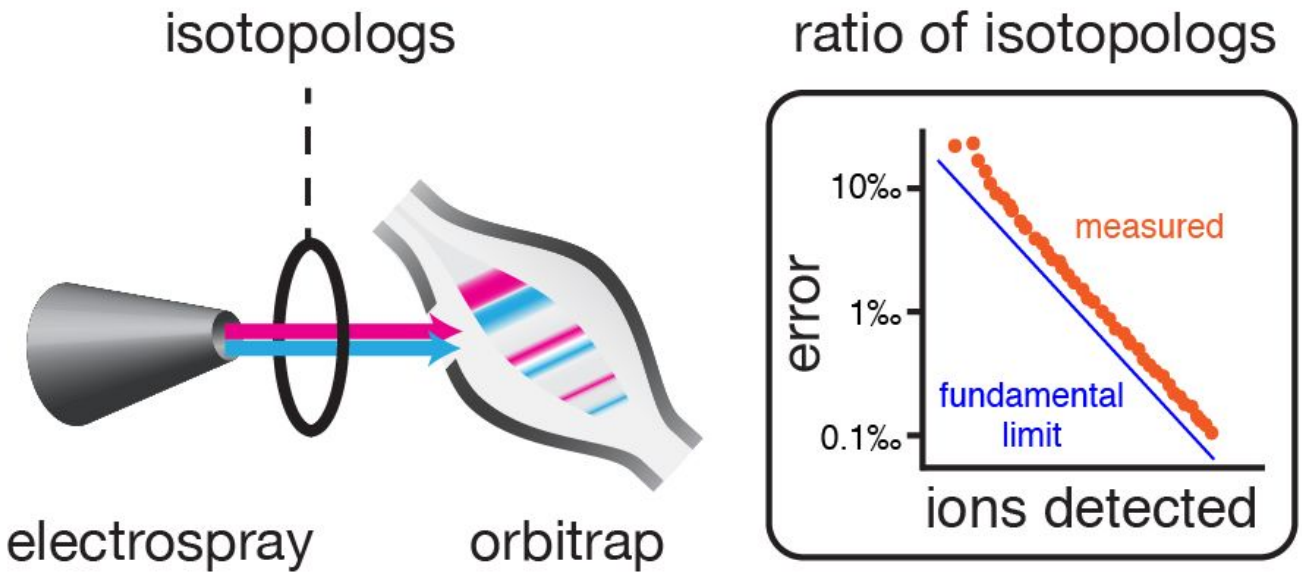

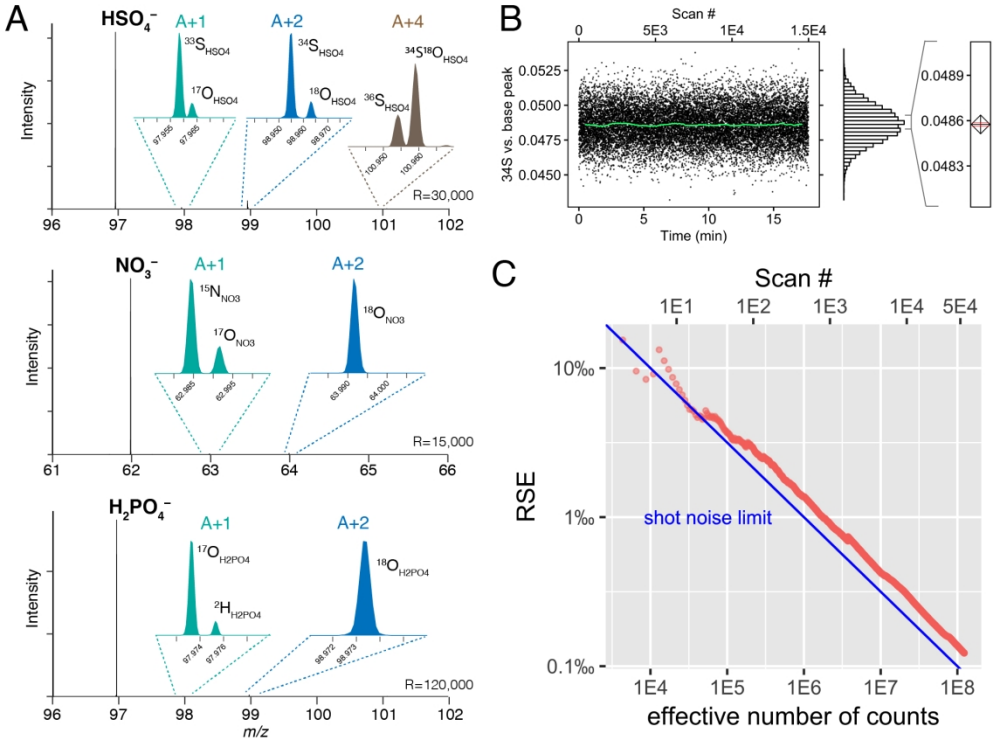

Fig. 1 Mass spectra and precision of isotope ratios. (A) Representative mass spectra of sulfate (HSO_4^-), nitrate (NO_3^-) and phosphate ions ($H_2PO_4^-$). The mass regions corresponding to A+1 (green), A+2 (blue) are magnified. Data for the low-abundance sulfate A+4 ions were collected by removing the base peak ($^1H^{32}S^{16}O_4^-$) using the quadrupole. (B) Ratio of the sulfate $^{34}S_{HSO4}$ isotopolog versus the base peak from a representative data collection (R = 30,000; 14 scans/s; AGC 3E5). The light green line represents the mean of a moving window of 1 min. The distribution of isotopolog ratios is symmetric and its geometric mean (0.04859; black diamond plus) can be determined with high precision (relative standard error (RSE) 1σ = 0.23 ‰; y-axis is magnified to better show the error bars in red). (C) The RSE of isotope ratios is approximately limited by counting statistics. The log-log plot shows the RSE (1σ) of the measurement of the $^{34}S_{HSO4}$ isotopolog versus the HSO_4^- base peak plotted against the effective number of counted ions. (Ref 23) For isotopologs a and b the number of effective counts $n_{eff}= (n_a*n_b)/(n_a+n_b)$. The blue line represents the shot-noise limit, $\sigma_{shot\ noise}=\sqrt{(1/n_{eff})}$.

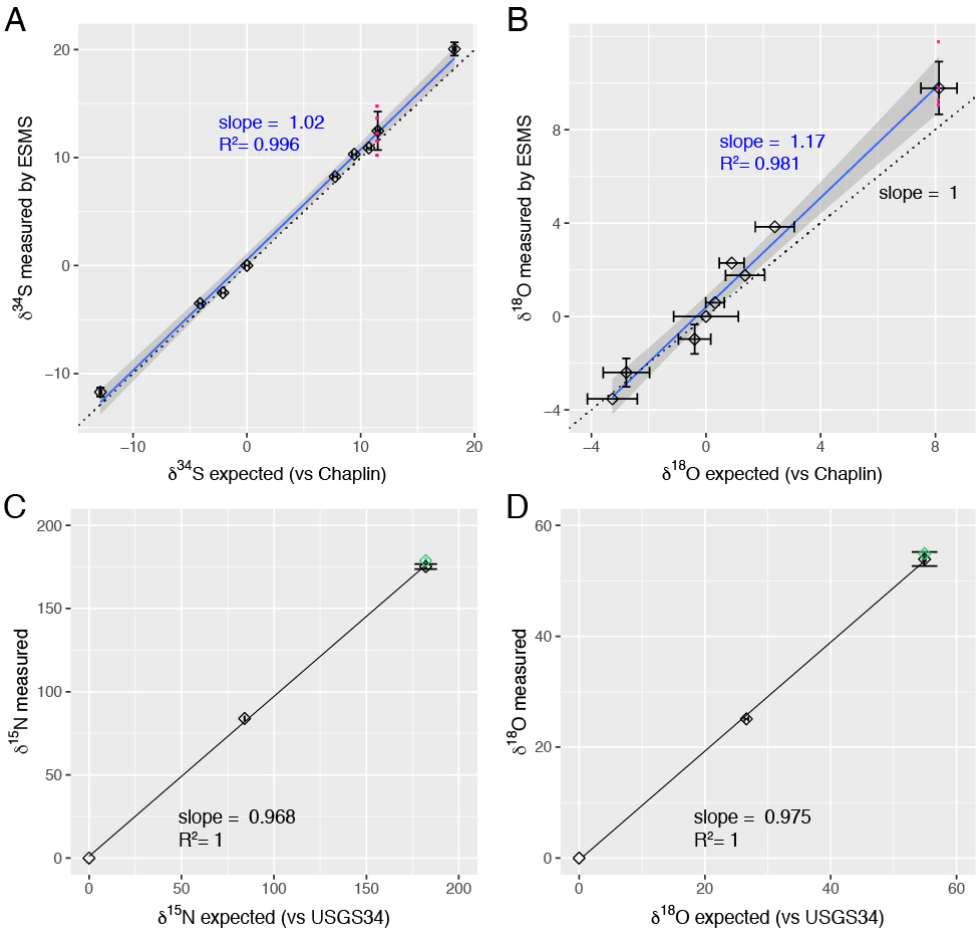

Fig. 2 Comparison of ESMS measurements with established IRMS methods. (A) Sulfate $\delta^{34}S$ from ESMS and combustion are highly correlated (Pearson's r > 0.994). The linear regression (blue) of the mean values has a slope close to 1 (95% confidence interval in grey). A dotted black line with slope = 1 is shown for comparison. Five independently measured data points for the Trona sample are shown as pink dots. Delta values are relative to sulfate from Chaplin, Canada (Table S2). (B) Sulfate $\delta^{18}O$ from ESMS and combustion are also highly correlated (Pearson's r > 0.990), but the linear regression has an increased slope when all replicates of the Trona sample (pink dots) are included in the analysis (slope 1.04, without without potential outlier). Note that the confidence interval (grey) does not include uncertainty associated with the expected δ value. (C) Nitrate $\delta^{15}N$ and (D) nitrate $\delta^{18}O$ measured by ESMS are highly correlated with independently known values for reference materials USGS32 and USGS34 and a 1:1 mixture of the two (Pearson's r = 0.999). Absolute $\delta^{18}O$ and $\delta^{15}N$ values from ESMS matched closely to the expected values. The isotopic difference was robustly detected also at a higher resolution (R = 30,000; green).

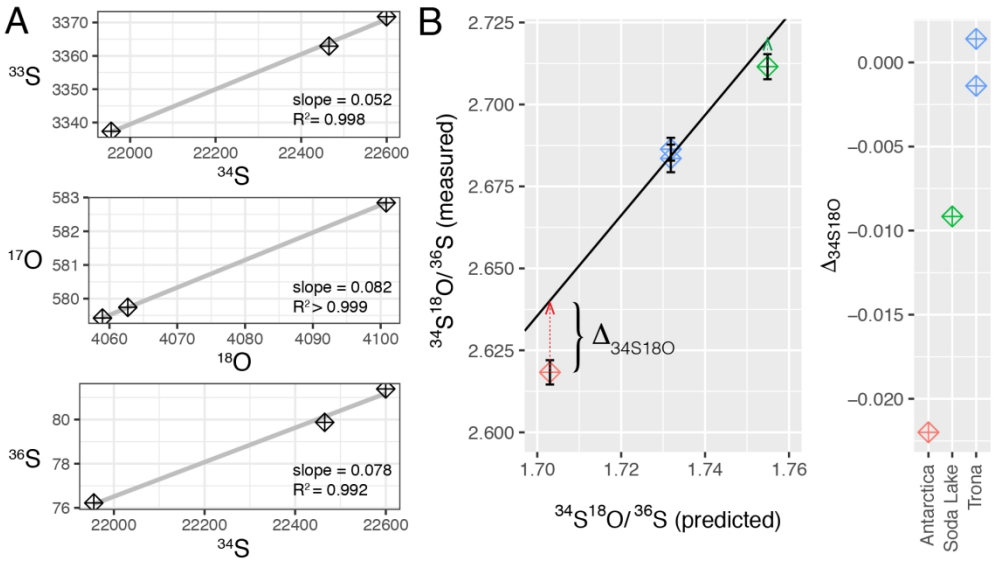

Fig. 3 Rare isotopologs of sulfate can be quantified with improved counting statistics by eliminating the base peak. (A) The ion counts per scan for $^{33}S_{HSO4}$, $^{34}S_{HSO4}$, and $^{36}S_{HSO4}$, as well as $^{17}O_{HSO4}$ and $^{18}O_{HSO4}$ are consistent with a near-linear relationship (R^2 >0.99), as expected for mass-dependent fractionation. (B) The signal of the clumped isotopolog $^{34}S^{18}O_{HSO4}$ varies between the tested sulfate materials. The black line represents a line of constant isotopic fractionation ($\alpha_{meas.-pred.}=R_{meas.}/R_{pred.}$; y-intercept = 0), defined by the average value of the Trona sample, which was measured at the beginning and end of data collection. Δ_{34S18O}, the difference between the measured $^{34}S^{18}O_{HSO4}$ / $^{36}S_{HSO4}$ and the extrapolated reference (black line), appears to indicate that the samples Soda Lake and Trona have a higher $^{34}S^{18}O$-clumping than Antarctica sulfate.

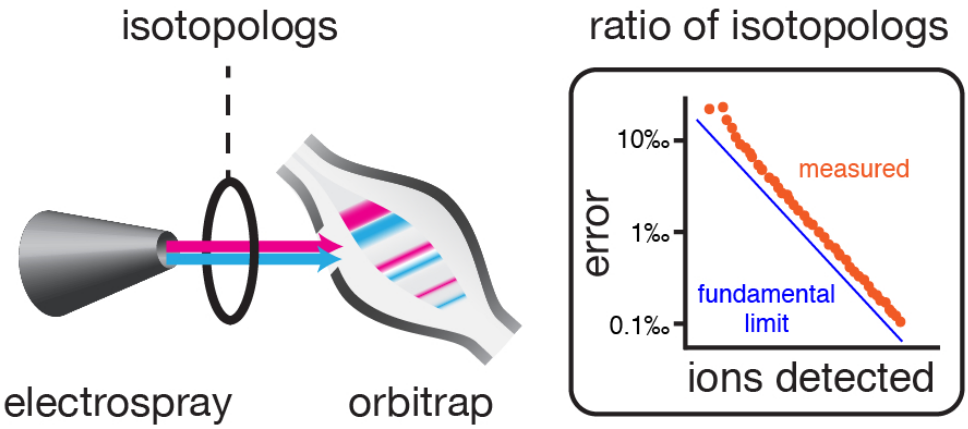
isotopologs
electrospray
orbitrap
ratio of isotopologs
10‰
1‰
0.1‰
error
measured
fundamental
limit
ions detected